SOME PHENOMENA OCCURRING IN n-TYPE INDIUM ANTIMONIDE EXPOSED TO HIGH FREQUENCY RADIATION

T. M. LIFSHITZ, Sh. M. KOGAN, A. N. VYSTAVKIN, and P. G. MEL'NIK

Institute of Electronics and Radio-Engineering U.S.S.R. Academy of Sciences

Submitted to JETP editor November 4, 1961

J. Exptl. Theoret. Phys. (U.S.S.R.) 42, 959-966 (April, 1962)

Experimental studies have been made on a number of phenomena which occur in n-type indium antimonide at helium temperatures, exposed to radiation in the millimeter range. The phenomena studied were photoconductivity and the appearance of an e.m.f. with and without the presence of a magnetic field. A semi-quantitative interpretation of the data obtained is given.

AMONG the well known semiconductor materials, n-type indium antimonide occupies a special position because of the very small effective mass of the carriers and their very high mobility. These properties of n-type InSb allow a whole series of phenomena in electrical and magnetic fields to be observed and studied more simply than in other materials. For n-type InSb at liquid helium temperature, magnetic fields of the order of one thousand oersted are already "strong." In electrical fields measured in fractions of a volt per centimeter, significant changes in mobility are already observed, together with the associated deviations from Ohm's law.[1] Recently there has been discussed in the literature the possibility of observing photoconductivity based on this effect, particularly in the short wavelength region of the radio frequency spectrum.[2,3] The aim of the present work is to clarify certain peculiarities of the phenomena which occur when n-type InSb cooled to 4.2° K is exposed to electromagnetic radiation of millimetric wavelength.

1. EXPERIMENTAL METHOD

The n-type InSb specimens studied were arranged in a helium cryostat at the end of a horn joined to a 4 mm wave guide (Fig. 1). The cryostat was situated between the poles of an electromagnet. The magnetic field could be directed both along the specimen axis and in a direction perpendicular to it. The specimen was exposed to a beam of 75 Gcs radiation, which was square-wave modulated at a frequency of 1000 cps. The radiation intensity in the plane of the specimen could be varied from zero to ~ 10^{-5} W/cm^2.

Polycrystalline n-type InSb specimens of dimensions 3.5 × 6 × 10 mm with soldered indium

FIG. 1. Schematic diagram of the placement of the specimen at the end of the horn carrying the high frequency power.
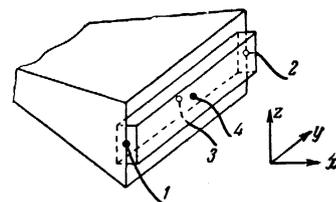
contacts were investigated. In the specimens studied, the carrier concentration at temperatures of 80° K and below was 6.5 × 10^{14} cm^{-3}, and their mobility was 4 × 10^4 cm^2/V-sec.

The alternating voltage picked off from the specimen was measured with a calibrated low-frequency amplifier. The magnitude and polarity of the signal could also be measured with the aid of a galvanometer.

2. EXPERIMENTAL RESULTS

Voltage-current characteristics. In Fig. 2 are given the voltage-current characteristics of a specimen for various magnitudes of transverse magnetic field, H.
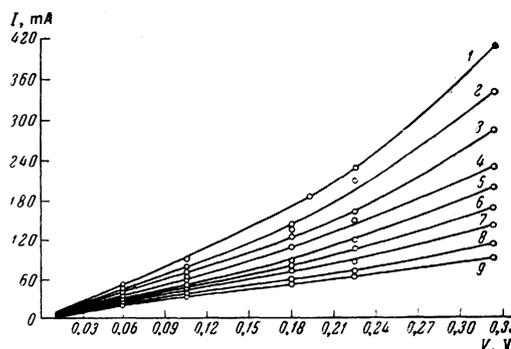

FIG. 2. Voltage-current characteristics for various strengths of applied magnetic field: 1−H = 0; 2−H = 800; 3−H = 1600; 4−H = 2400; 5−H = 3200; 6−H = 4000; 7−H = 4800; 8−H = 5600; 9−H = 6400 Oe.

For not too small electrical fields, the conductivity increases with increasing field. This agrees with the assumption that the predominant scattering mechanism for carriers in n-type InSb at T = 4.2° K is ionized impurity scattering. For very small fields, the nonlinearity of the voltage-current characteristic is of opposite sign, and the point of inflection of the characteristic is displaced along the voltage axis towards larger E as the magnetic field increases. The nature of the phenomena leading to such a form of the characteristic for limitingly small fields is not clear at the present time. It is possible that the polycrystallinity of the specimens or contact phenomena are involved here. In the present work we limit consideration to phenomena in static and high frequency fields δ such that the nonlinearity characterized by the quantity

$$\beta \equiv [\sigma (E)]^{-1} d\sigma/dE^2 \tag{1}$$

is positive ($\sigma(E)$ is the specific electrical conductivity in the field E).

The variation of β with E for various values of the field H is given in Fig. 3. It is seen that, as H increases, β diminishes.
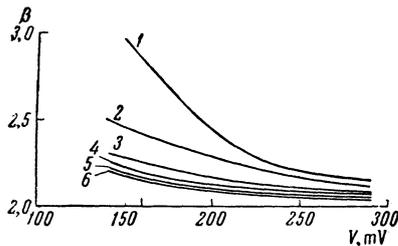

FIG. 3. The variation of β with applied voltage for various values of magnetic field : 1—H = 0; 2—H = 1000; 3—H = 2000; 4—H = 3000; 5—H = 4000; 6—H = 5400 Oe.

The signal in the absence of a magnetic field. On irradiating the specimen in zero external electrical and magnetic fields, no voltage was observed between electrodes 1 and 2 (Fig. 1). Meanwhile, irradiation produced between contacts 3 and 4 an e.m.f., with a direction such as to make positive the electrode 3, which was on the irradiated side of the specimen. By observing the e.m.f. pulses on an oscilloscope, it could be seen that their shape was the same as the shape of the pulses of incident radiation (there was no significant distortion of the fronts and tops of the pulses). It is of interest to note that an even greater e.m.f. was also observed between electrodes 3 or 4 and either of electrodes 1 or 2; in this case the central electrode (3 or 4) was always positive.

An alternating voltage signal could be observed between electrodes 1 and 2 when an external elec-
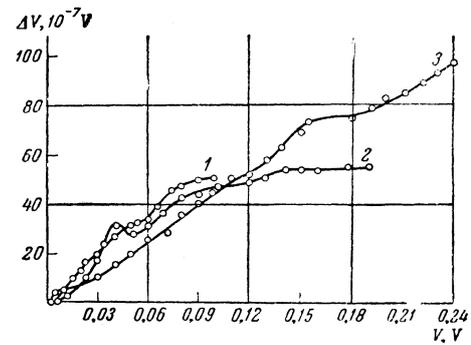

FIG. 4. The variation of photo-response ΔV with the voltage applied to the specimen for various magnetic fields: 1—H = 0; 2—H = 3200; 3—H = 5100 Oe.

trical field was applied to them. The signal amplitude (photoresponse) increased with applied field (see Fig. 4, curve 1) for fields up to about 0.1 V/cm. On further increasing the field, the voltage on the specimen decreased abruptly (by ~10—20%), and irregular oscillations of large amplitude arose in the circuit. The voltage at which these phenomena are observed can be called the signal break point.

The signal in the presence of a magnetic field. On applying a magnetic field, a signal, i.e., an alternating e.m.f., could be observed in zero external electrical field. The form of the signal was the same as in the cases described above. The amplitude of the signal increases from zero and changes non-monotonically with increasing magnetic field, passing through one or more maxima and minima (curve 1, Fig. 5). The same non-monotonic behavior of the signal with increasing magnetic field is also observed when an external voltage E = 0.1 V/cm is applied to the specimen (curve 2, Fig. 5). In this case the value of the signal was close to its maximum value on curve 1.

If the direction of the magnetic field H coincides with the axis of the specimen along which the external electrical field is applied, the variation of the signal with H is essentially different (Fig. 6) — the variation being basically monotonic. Small irregularities in the experimental curve can, apparently, be associated with the presence of a
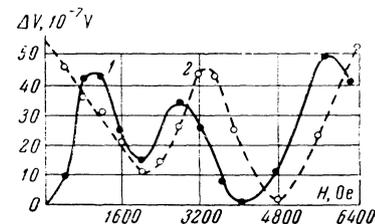

FIG. 5. The dependence of photo-response ΔV on the applied transverse magnetic field: 1—with zero external electric field; 2—with an external electric field.
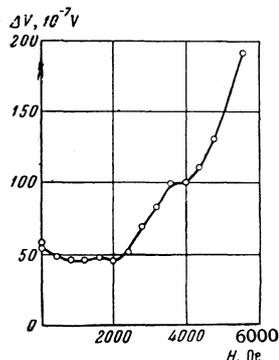
FIG. 6. The dependence of the photo-response ΔV on the magnetic field applied along the specimen axis.
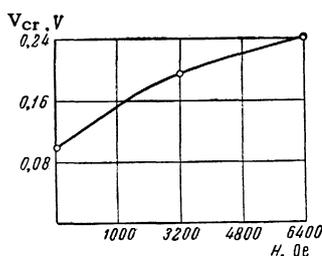

FIG. 7. The dependence of the signal break voltage on the applied magnetic field (the curve corresponds to the end points of the curves in Fig. 4).

small transverse component of the magnetic field, due to inexact alignment of the vector **H** with the axis of the specimen.

Curves analogous to curve 1 of Fig. 4 were also taken for various values of transverse magnetic field. As seen from Fig. 7, the signal break point is displaced to increased voltages as the magnetic field increases.

3. DISCUSSION OF THE RESULTS

We enumerate the physical phenomena which might conceivably form the basis for the effects we observed: a) a bolometric effect (heating of the specimen by the radiation); b) an impurity photoeffect; c) phenomena at contacts and crystallite boundaries; d) a change of the energy distribution function of conduction electrons — "heating" of the electron gas by the radiation.

We consider each of the mechanisms specified.

a) The phenomena observed cannot be attributed to heating of the specimen by the radiation for two reasons: first, the time lag of the photo-response was smaller than 10^{-4} sec; second, the radiant energy absorbed in the specimen in a time of 10^{-4} sec is too small to cause a signal of the observed size.

b) As is well known, for zero and weak magnetic fields (less than 4×10^3 Oe), and for impurity concentrations greater than 5×10^{13} cm^{-3}, all shallow donor impurities are ionized.[4-6] Measurements of the Hall effect, on the specimens we studied, show that the carrier concentration does not change with magnetic field in the entire range

of fields up to 6000 Oe, i.e., in this range of fields all the donor centers remain ionized, and an impurity photoeffect cannot take place.

The signal (e.m.f.) observed in a magnetic field for V = 0 cannot in general be explained by an impurity photoeffect. In fact, such a signal could arise due to the impurity photoelectromagnetic (PEM) effect. The required gradient of carrier concentration in a direction perpendicular to the magnetic field could occur due to absorption of radiation in the specimen. Absorption is bound to occur due to free carriers (it is estimated that in our conditions the absorption coefficient is ~ 200 cm^{-1}). It follows from general physical considerations that a stationary impurity PEM effect is impossible. We estimated the nonstationary impurity PEM effect which occurs when the radiation intensity changes with time. It was found that the effect depends on the value of the recombination time and also on the time taken to establish space charge, which is equal to L^2/D, where L is the Debye screening length, and D is the diffusion coefficient. Both times are at most several orders smaller than the modulation period (10^{-3} sec). However, experiment shows that throughout an entire half-cycle the effect is steady and no "spikes" of e.m.f. corresponding to the fronts of the radiation are observed.

c) The role of contacts in the phenomena observed is not clear. However, when the geometry of the contacts and the high frequency of the radiation is taken into consideration, it is difficult to suppose that these phenomena can, to any significant degree, be due to detection at contacts. It is still more difficult to maintain that detection occurred at the grain boundaries, since the specimen was coarse-grained.

d) It is well known that in an electric field (including the field of the electric vector of an electromagnetic wave) the distribution function of conduction electrons with respect to energy [more accurately, the symmetrical part of the distribution function $f_0 (\epsilon)$] changes relative to the equilibrium Fermi function. This change in $f_0 (\epsilon)$ can, under certain conditions, be regarded as an increase in the "electronic temperature" T relative to the lattice temperature T_0. The concept of "heating" the electron gas by radiation permits the basic results we obtained to be explained consistently and naturally.

In fact, on heating the electron gas with radiation the carrier mobility changes, and this, in turn, changes the conductivity of the specimen. Whereas a change of carrier concentration due to radiation

without a mobility change is the usual basis of photoconductivity, in our case, to the contrary, the photoconductivity is caused by a carrier mobility change with no change of concentration.

From this point of view, the appearance of an e.m.f. in a magnetic field is also understandable. This e.m.f. is nothing more than the e.m.f. of the "electronic" thermomagnetic effect (the analogue of the Nernst-Ettinghausen e.m.f.), arising because a gradient of electron temperature exists in the specimen.

Let us consider in more detail the phenomena of carrier heating in n-type InSb under the conditions of the experiment.

The major mechanism of conduction electron scattering at 4.2° K in n-type InSb specimens is scattering at charged impurity centers. Starting from the values of mobility given above, and taking the effective mass as $m = 1.3 \times 10^{-2} m_0$,[7] we can easily estimate the momentum relaxation time: $\tau_p \sim 10^{-12}$ sec. Calculation, which can be made in accordance with the results of [8], shows that the frequency of inter-electronic collisions is $\tau_{nn}^{-1} \sim 10^{12}$ sec^{-1}. It will be shown below that the relaxation time for electron energy τ_e is significantly larger than τ_{nn}. We can, therefore, assume that the function $f_0 (\epsilon)$ has a Fermi form with electron temperature $T > T_0$:

$$f_0 (\epsilon) = [e^{(\epsilon - \zeta)/T} + 1]^{-1} \tag{2}$$

(here and below T denotes the temperature in energy units).

When heating of the electron gas is small, i.e.,

$$(T - T_0)/T_0 \ll 1,$$

the power transferred by the electrons to the lattice is proportional to the difference $\Delta T = T - T_0$:

$$P_{e \to lat.} = n (d\bar{\epsilon}/dT) (\Delta T/\tau_e), \tag{3}$$

where $\bar{\epsilon}$ is the mean energy of the electrons. To evaluate the time τ_e, we can use the experimental data on the variation of the static mobility with field, i.e., the deviations of the voltage-current characteristic from ohmic. In not very strong fields E the mobility is

$$\mu = \mu_0 (1 + \beta E^2). \tag{4}$$

Using the energy balance equation

$$e\mu n E^2 - n (d\bar{\epsilon}/dT) (\Delta T/\tau_e) = 0, \tag{5}$$

we find that in weak static fields

$$\Delta T = [e\mu_0 \tau_e/(d\bar{\epsilon}/dT)] E^2. \tag{5a}$$

Therefore,

$$\frac{\Delta\mu}{\mu_0} = \frac{1}{\mu_0} \left(\frac{d\mu}{dT}\right)_{T_0} \Delta T = \frac{e\tau_e (d\mu/dT)_{T_0}}{(d\bar{\epsilon}/dT)} E^2. \tag{6}$$

Comparing (6) and (4), we obtain

$$\tau_e = \beta (d\bar{\epsilon}/dT)/e (d\mu/dT). \tag{7}$$

Calculation shows that in the specimens studied $d\bar{\epsilon}/dT \sim 1$ and

$$(d\mu/dT)_{T_0} \sim \mu/T_0.$$

Therefore,

$$\tau_e \sim \beta T_0/e\mu_0. \tag{8}$$

In the absence of magnetic field we obtain $\beta \sim 1 (V/cm)^{-2}$. Hence,

$$\tau_e \sim 10^{-8} \text{sec}. \tag{9}$$

The introduction of the concept of an electronic temperature simplifies quantitative calculations, although, of course, the basic qualitative conclusions can also be obtained without the use of this concept.

We shall consider the experimental results presented above from the viewpoint described.

The photo-response in zero magnetic field. The relative change of voltage on the specimen is

$$\frac{\Delta V}{V} = -\frac{1}{2} \frac{\Delta R}{R} = \frac{1}{2l} \int_0^l dx \frac{\Delta\mu (x)}{\mu} = \frac{d\mu/dT}{2\mu_0 l} \int_0^l dx \Delta T (x). \tag{10}$$

When calculating the value of ΔT we must bear in mind two facts. Firstly, in the specimen studied

$$\omega\tau_p = 5 \cdot 10^{11} \text{sec}^{-1}\tau_p \lessgtr 1. \tag{11}$$

Therefore, the real part of the electrical conductivity $\sigma' (\omega)$ differs little from its static value $\sigma (0)$. Secondly,

$$\omega\tau_e \gg 1, \tag{12}$$

and, therefore, oscillations of the electronic temperature with frequency 2ω can be neglected, and it can be considered that T is determined by the intensity of radiation at a given moment. If $\overline{E^2}$ is the mean value of the high frequency field, then ΔT is given by the equation

$$\sigma (0) \overline{E^2} - n \frac{d\bar{\epsilon}/dT}{\tau_e} \Delta T = 0. \tag{13}$$

Whence it follows

$$\Delta T = \frac{e\mu_0 \tau_e}{d\bar{\epsilon}/dT} \overline{E^2}, \tag{14}$$

$$\frac{\Delta V}{V} = \frac{e\tau_e (d\mu/dT)}{2 (d\bar{\epsilon}/dT)} \frac{1}{l} \int_0^l \overline{E^2} (x) dx = \frac{\beta}{2l} \int_0^l dx \overline{E^2} (x). \tag{15}$$

In writing down Eq. (13) and obtaining (14) for ΔT, we have neglected the electronic thermal conduc-

tivity which tends to equalize the electronic temperature at points of different field intensity.
There is no difficulty in including the thermal conductivity approximately, but it does not change formula (15) for the photo-response.

It is also useful to write down the expression for the photo-response in terms of the intensity of the incident wave J_0, for the case when a plane electromagnetic wave falls on a specimen, the dimensions of which, in directions perpendicular to the direction of incidence, are small in comparison with the wavelength:

$$\frac{\Delta V}{V} = \frac{8\pi}{c}\,\beta\,\frac{J_0}{(n+1)^2+\varkappa^2}\,\frac{1}{Kl}\,A\,(n,\varkappa,\lambda,l). \qquad (16)$$

Here n and κ are the indices of refraction and absorption, and $K = (4\pi\kappa/\lambda)$ is the absorption coefficient,

$$A\,(n,\varkappa,\lambda,l) = \frac{e^{Kl}-1+R_R(1-e^{-Kl})-2Kl\sqrt{R_R}[\sin(4\pi nl\lambda^{-1}+\psi)-\sin\psi]/(4\pi nl/\lambda)}{e^{Kl}+R_R^2\,e^{-Kl}-2R_R\cos(4\pi nl/\lambda+2\psi)}, \qquad (17)$$

where $R_R = [(n-1)^2+\kappa^2]/[(n+1)^2+\kappa^2]$ is the reflection coefficient of the material, and

$$\tan\psi = 2\varkappa/(n^2+\varkappa^2-1). \qquad (18)$$

For $Kl \gg 1$ the value of $A(n,\kappa,\lambda,l) \approx 1$. We shall evaluate the magnitude of the signal ΔV for a radiation intensity of $J_0 = 10^{-5}$ W/cm^2 and V = 0.1 V. From Fig. 3 we find: $\beta \approx 3\,(V/cm)^{-2}$.

If we evaluate the quantities K, n and κ by means of the well known formulae for the complex dielectric constant of an electron gas $\epsilon\,(\omega)$,[19] we obtain

$$K \approx 200 \text{ cm}^{-1},$$

$$(n+1)^2+\varkappa^2 = 100. \qquad (19)$$

This gives for the magnitude of this signal a value of 3×10^{-7} V, which agrees in order of magnitude with the experimental data.

We note that the formulae cited for $\epsilon\,(\omega)$ were obtained by a method using the kinetic equation, and, strictly speaking, are invalid under the conditions of interest to us (in our case $\hbar/\tau_p \gtrsim \bar\epsilon$, whereas the condition for the applicability of the classical kinetic equation method is the inequality $\hbar/\tau_p \ll \bar\epsilon$). However, calculations show that, because in the calculation we used the experimental value $\sigma(0)$, the order of magnitude of

$$K\,[(n+1)^2+\varkappa^2],$$

appearing in (16) (when $Kl \gg 1$) is correct.

From the viewpoint of heating the electron gas, the appearance of an e.m.f. between the irradiated side of the specimen and the opposite side is reasonable. This e.m.f. is none other than an "electronic" thermo-e.m.f., which arises because of the difference in electronic temperature between the two sides. Such an interpretation also agrees with the observed polarity of this e.m.f. The appearance of a thermal e.m.f. between the center of the specimen and either of the electrodes 1 or 2 is related to the fact that the maximum intensity of the high-frequency field is at the center of the specimen, whereas the intensity falls off symmetrically towards the ends of the specimen.

The e.m.f. in a magnetic field. We estimate the magnitude of the "electronic" thermomagnetic (transverse) Nernst-Ettinghausen effect. For small magnetic fields when $\mu H/c \ll 1$ (under our conditions for $H \ll 10^3$ Oe), the transverse Nernst-Ettinghausen field is in order of magnitude

$$E_y \sim \frac{T_0}{e}\,\frac{\mu H}{c}\,\frac{T(0)-T(x)}{T_0 x}, \qquad (20)$$

where T(x) is the electronic temperature at depth x. When

$$\Delta T\,(x) = \Delta T\,(0)e^{-Kx},$$

the value of E_y can be related to the magnitude of the photo-response in zero magnetic field:

$$E_y \sim \frac{T_0}{e}\,\frac{\mu H}{c}\,2K\left(\frac{T}{\mu}\,\frac{d\mu}{dT}\right)^{-1}\frac{\Delta V}{V}. \qquad (21)$$

This variation agrees with experimental data for E_y and ΔV in the range of small magnetic fields. The problem of the variation of signal with magnetic field for large fields must be the subject of special consideration.

The authors express their gratitude to L. Ya. Kroll and V. S. Ivleva for the gift of the specimens.

[1] R. J. Sladek, Phys. Rev. 120, 1589 (1960).
[2] B. V. Rollin, Proc. Phys. Soc. (London) 77, 1102 (1961).
[3] T. S. Moss, Programme of the 1961 International Conference on Photoconductivity, Ithaca, N. Y., 1961, p. 7; J. Phys. Chem. Solids 22, 117 (1961).
[4] R. W. Keyes and R. J. Sladek, J. Phys. Chem. Solids 1, 143 (1956).
[5] E. H. Putley, Proc. Phys. Soc. (London) 73, 280 (1959).
[6] E. H. Putley, Proc. Phys. Soc. (London) 76, 802 (1960).

[7] H. Welker and H. Weiss, Solid State Physics **3**, Academic Press, Inc., N. Y., 1956, p. 1.

[8] H. Fröhlich and B. V. Paranjape, Proc. Phys. Soc. (London) **B69**, 21 (1956); R. Stratton, Proc. Roy. Soc. (London) **A242**, 355 (1957).

[9] T. Moss, The Optical Properties of Semiconductors, Butterworths, London, 1959, Chap. II, Section 5.

Translated by K. F. Hulme

158

THE CONTRIBUTION OF COLLECTIVE MOTION TO THE LIFTING OF l-FORBIDDENESS

É. E. BERLOVICH, Yu. K. GUSEV, V. V. IL'IN, V. V. NIKITIN, and M. K. NIKITIN

Leningrad Physico-technical Institute, Academy of Sciences, U.S.S.R.

Submitted to JETP editor November 11, 1961

J. Exptl. Theoret. Phys. (U.S.S.R.) 42, 967-972 (April, 1962)

The lifetimes of M1 transitions of the type $g_{7/2} \rightarrow d_{5/2}$ have been studied in the spherical nuclei Eu^{147}, Eu^{149}, and Eu^{151}, which just precede the deformation region. The half-lives of the first excited states ($g_{7/2}$) of these three nuclei are equal respectively to $(1.8 \pm 0.2) \times 10^{-10}$, $(3.2 \pm 0.2) \times 10^{-10}$ and $(3.4 \pm 0.2) \times 10^{-9}$ sec, and the M1 delay factors are 115, 78, 47, in contrast to the average value of ~ 300 for other known single-proton M1 transitions which are l-forbidden. The small values of the observed delay factors and their monotonic decrease as we approach the deformation region seem to indicate an increasing contribution of the collective motion and a corresponding weakening of the l-forbiddenness.

1. INTRODUCTION

IN a preceding paper[1] the lifetimes of corresponding $h_{11/2}$ levels in the spherical nuclei Eu^{147}, Eu^{149} and Eu^{151} were studied, and it was shown that the matrix elements for M2 and E3 radiative transitions change smoothly when a pair of neutrons is added. In the present work we have investigated the lifetimes of first excited states of these same nuclei, which in all three cases give rise to protonic M1 transitions of the type $g_{7/2} \rightarrow d_{5/2}$, which are forbidden by the angular momentum selection rule ($\Delta l = 2$).

In all known cases, l-forbidden M1 transitions have been observed near closed shells, and the values of the delay factors for proton transitions group very well around the average value $\bar{F} = \tau_{exp}/\tau_{Weissk.} = 300$; at the same time the probabilities for allowed proton transitions ($\Delta l = 0$) agree much better with the single-particle Weisskopf estimates (the F factor is small).

In the literature various types of nucleon interaction have been considered as causing the occurrence of l-forbidden transitions: meson-exchange interaction,[2] spin-exchange interaction,[3] spin-exchange coupling,[4] etc. The most successful treatment is that based on the assumption that l-forbidden transitions appear because of configuration mixing in the initial or final state of the radiating particle.[5] Since l-forbidden transitions are observed in the immediate vicinity of closed shells, it was natural to assume that the collective effects which are treated in the unified model of the nucleus[6] should not play an important part in the lifting of the forbiddenness.

The nuclei studied in the present work lie just before the region of large deformations, where collective motion manifests itself most strongly. One might expect that the influence of collective effects would significantly affect the probabilities of l-forbidden transitions even for neutron numbers below the critical value (N = 89), where the equilibrium shape is still spherical.

2. DESCRIPTION OF EXPERIMENTS

The 229.5-keV transition in Eu^{147}. To study the lifetime of the 229.5-keV level in Eu^{147}, we used the gadolinium fraction separated from a tantalum target[1] irradiated for two hours with 660-MeV protons in the Joint Institute synchrocyclotron. During the first few days after irradiation, the 35 hour activity of Gd^{147} predominated, converting to Eu^{147} by electron capture. The measurements were made with a multichannel time analyzer using time to pulse height conversion[7] and a two-crystal scintillation spectrometer with sodium iodide crystals (d = 40 mm, h = 30 mm), and a type FÉU-33 photomultiplier.

The "windows" of the scintillation spectrometer were set on the photopeak of the cascades formed by the 396- and 229.5-keV γ quanta, the exact setting of the windows being determined by a preliminary study of coincidences when one "window" is left fixed and the window in the other channel is varied. To reduce the load on the FÉU photomultiplier, the characteristic x radiation was reduced by a phosphor bronze filter. The lifetime of the level was determined from the shift of the center of gravity of the coincidence curve[8] relative to the reference curve for "prompt" coinci-
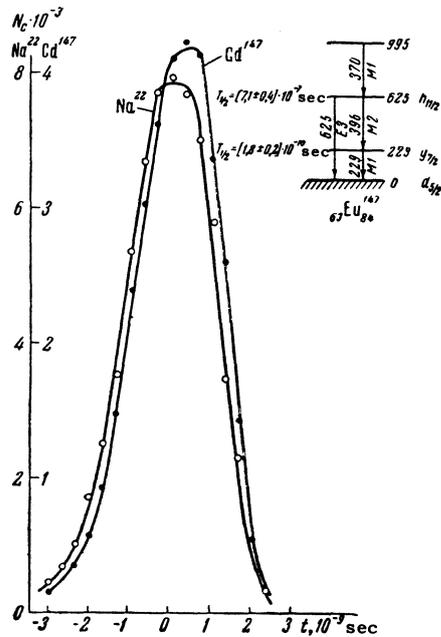
FIG. 1. Coincidence curves (one of six series) for sources of Gd^{147} (decay scheme shown in insert) and Na^{22}, taken with a pair of NaI (Tl) crystals with the same energy intervals.

FIG. 2. Coincidence curves (one of five series) for Gd^{149} and Co^{60} sources, taken with a pair of stilbene crystals.

dences, which was obtained by recording the annihilation quanta from a Na^{22} source (Fig. 1). A correction (~5%) was made to the value of the shift for the contribution of "fast" coincidences, which correspond to hard γ transitions in Eu^{147} and Sm^{146}, which give "tails" of their Compton distributions in the region of the photopeaks from the 229.5- and 396-keV γ quanta.

The half-life was found to be

$$T_{1/2} = (1.8 \pm 0.2) \cdot 10^{-10} \text{ sec.}$$

The 150-keV transition in Eu^{149}. Nine to ten days after irradiation, when the Gd^{147} had practically all decayed, we carried out a chromatographic purification of the source of the accumulating Eu^{147} with a period of 24 days and other isotopes of europium. The remaining activity was due mainly to Gd^{149}, which converts to Eu^{149} with a half-life of 9.3 days by electron capture. Since the 150-keV transition has a sizable conversion coefficient (total conversion coefficient $\alpha_{tot} = 0.63$), to improve the time resolution it was convenient to use a thin crystal of stilbene (~0.5 mm) for recording the coincidences between the conversion electrons from this transition and the cascade γ rays at 346 keV, which were recorded at their photopeak in a sodium iodide crystal. To obtain a reference curve, $\beta\gamma$ coincidences were taken with a Co^{60} source, and the lifetime of the 150 keV level was determined from the shift of the center of gravity of the coin-
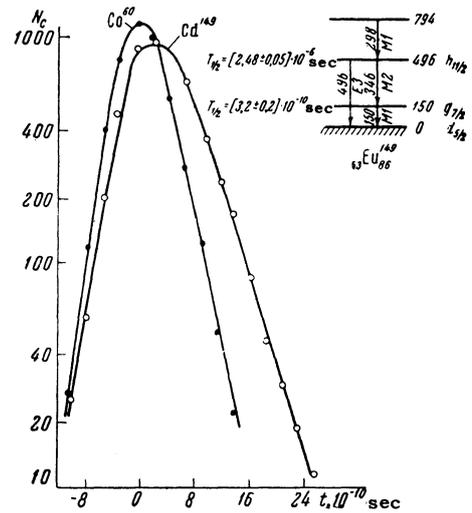
cidence curves obtained with Gd^{149} and Co^{60}. In another variant of the experiment, 346-keV γ rays were recorded using a packaged stilbene crystal (d = 35 mm, h = 20 mm); this permitted an improvement of the time resolution to such an extent ($2\tau_0 \sim 10^{-9}$ sec) that the exponential shape began to be apparent on the right side of the coincidence curve for the Gd^{149} source (Fig. 2). Treating this branch of the curve by least squares gave

$$T_{1/2} = (3.2 \pm 0.2) \cdot 10^{-10} \text{ sec.}$$

This result coincided with the average value from numerous measurements using the center of gravity method.

The 21.7-keV transition in Eu^{151}. The source of Gd^{151}, which decays by electron capture to Eu^{151} with a period of ~170 days, was obtained by separation from the terbium fraction (the irradiation time of the tantalum target in the proton beam was ~4 hours), 25—30 hours after the irradiation, when most of the Tb^{151} nuclei ($T_{1/2}$ = 20 h) have converted to Gd^{151}, while the Tb^{153}, which decays with a half-life of 60 h to Gd^{153}, has only partially decayed. This improved the ratio of Gd^{151} to Gd^{153} ($T_{1/2}$ = 230 d) in our source in favor of Gd^{151}.

For the measurements we used a two-crystal scintillation coincidence spectrometer with a variable delay line.[9,10] The multichannel time analyzer could not be used in this case because of the limited region of linearity, which prevented us from following the decay curve over several periods.

Coincidences were recorded between the K conversion electrons from the 175-keV transition (α_K = 2.5) and the L, M, and N electrons from